A case study analysis of a landslide considering the residual shear strength of unsaturated soil

Xiuhan Yang & Sai K. Vanapalli
Department of Civil Engineering – University of Ottawa, Ottawa, Ontario, Canada

ABSTRACT
Several of the natural and compacted fine-grained soils slopes that are in either saturated or unsaturated condition typically undergo a large deformation prior to reaching failure conditions. Such slopes should be designed taking account of their strain-softening behavior based on their residual shear strength parameters. In this paper, a recently reactivated Outang landslide near the Three Gorges Dam in China is interpreted using the residual shear strength parameters of unsaturated soils. A series of site investigations (i.e., boreholes, exploratory wells and trenches, footrill) and direct shear tests results were used to study the progressive failure behavior of this landslide. Slope stability analyses were conducted using Geoslope considering the combined influence of the precipitation and Yangtze River water level variation, based on the residual shear strength parameters. This study might be of significant interest to the geotechnical engineers to understand the unsaturated soil slope behavior at residual state.

RÉSUMÉ
La plupart des pentes naturelles et compactes des sols à grains fins, saturées ou non saturées, subissent généralement une déformation importante avant d'atteindre les conditions de rupture. Ces pentes doivent être conçues en tenant compte de leur comportement d'adoucissement des contraintes en fonction de leurs paramètres de résistance au cisaillement résiduelle. Dans cet article, un glissement de terrain d'Outang récemment réactivé près du barrage des Trois Gorges en Chine est interprété à l'aide des paramètres de résistance au cisaillement résiduel des sols non saturés. Une série d'études de site et de résultats d'essais de cisaillement direct ont été utilisés pour étudier le comportement progressif en cas de défaillance de ce glissement de terrain. Sur la base de la résistance au cisaillement résiduelle, une série d'analyses de stabilité de la pente ont été effectuées à l'aide de Geoslope, en tenant compte de l'influence combinée des précipitations et de la variation du niveau de l'eau du fleuve Yangtze. Cette étude présente un intérêt considérable pour les ingénieurs géotechniques afin de comprendre les comportements de la pente non saturée à l'état résiduel.

1 INTRODUCTION

The soil slopes that are in a state of unsaturated condition typically undergo a large deformation prior to reaching failure conditions. However, there are limited number of case studies in the literature (Widger & Fredlund 1979; Yang et al. 2017) that highlight this behavior. In these case studies, the soil shear strength on the sliding zone drops after reaching the peak shear strength (PSS) due to the large shear deformation until it reaches a residual value. The reduction in shear strength resulting from the large shear deformation is widely referred to in the literature as strain-softening behavior (Skempton, 1964). The minimum shear strength is referred to as the residual shear strength (RSS).

Many researchers have highlighted the role of RSS in the long-term slope stability analysis of saturated fine-grained soil slopes (Potts et al. 1997; Locat et al. 2013). These studies suggest that the magnitudes of shear strength due to the shear deformation zone are different along the sliding slope. The shear strength of the soils reduces due to strain-softening behavior in the sliding zones that underwent large deformation. The factor of safety (FOS) would be overrated if the slope stability analysis is based on the PSS parameters. This is due to the reason that the RSS which governs the slope failure is typically lower than the PSS. More recently, Qi and Vanapalli (2016) highlighted the importance of RSS in the slope stability analysis of unsaturated expansive soils. Therefore, the strain-softening behavior based on RSS must be considered for the reliable modelling, analysis and design of the unsaturated slopes which can undergo large shear deformation prior to reaching the failure condition.

The RSS behavior of saturated soils has been widely investigated in the literature. Skempton (1964) was the first investigator who recognized the importance of RSS in long-term slope stability. Lupini et al. (1981) analyzed the failure mechanism of saturated soils associated with the RSS. In recent years, the RSS behavior of unsaturated soils was investigated from experimental studies by some researchers (Infante Sedano & Vanapalli 2011; Hoyos et al. 2014; Romero et al. 2014). The experimental results have highlighted that the matric suction has a significant influence on the RSS and strain-softening behavior of unsaturated soils. However, limited experimental data on the RSS of unsaturated soils is presently available in the literature. More importantly, studies related to simple yet reliable approaches for predicting the RSS of unsaturated soils are lacking.

Infante Sedano & Vanapalli (2011) proposed a model for predicting the residual shear strength of unsaturated soils, which is summarized below:

$$\tau_r = c_r' + \left(\sigma_n - u_a\right)\tan\phi_r' + \left(u_a - u_w\right)(S^{\kappa_r})\tan\phi_r' \qquad [1]$$

Where, $(\sigma_n - u_a)$ is the net normal stress; $(u_a - u_w)$ is the matric suction; c_r' and ϕ_r' are the residual shear strength parameters of saturated soils; S is the degree of saturation; κ_r is the fitting parameters.

Reasonably good comparisons were observed between the predicted results and experimental results of suction-controlled modified ring shear tests conducted on unsaturated soils. However, S in this model was suggested to be estimated from an apparent soil-water characteristic curve (SWCC) determined on sheared specimens. In other words, a specimen which has been sheared to the residual state should be used to obtain the SWCC using the conventional pressure plate apparatus. The S in Eq. 1 can be estimated from the apparent SWCC equation based on the matric suction value. However, it is time consuming for measuring such a SWCC.

In order to simplify the required input parameters, Yang & Vanapalli (2018) proposed a new model to predict the RSS of unsaturated soils, which is based on the conventional SWCC. In this model, the residual shear strength of unsaturated soils can be expressed as:

$$\tau_r = c_r' + \left(\sigma_n - u_a\right)\tan\phi_r' + \left(u_a - u_w\right)\left(\frac{\theta - \theta_i}{\theta_s - \theta_i}\right)^{\kappa_r}\tan\phi_r' \qquad [2]$$

Where, θ_s is the saturated volumetric water content; θ_i is the volumetric water content corresponding to the inflection point (i.e. the peak point of the derived function curve of SWCC equation, as shown in Figure 1); κ_r is the fitting parameter for RSS, which is suggested to be 0.4 for Indian Head till; which is a glacial till from Saskatchewan, Canada.

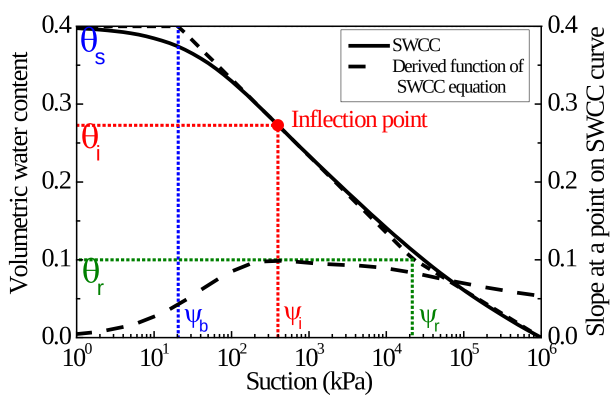

Figure 1 The salient features of the soil-water characteristic curve (SWCC)

This RSS prediction model requires only the information of a conventional SWCC which can be obtained relatively easily from the laboratory. However, this model can only be applied within a relatively low suction range, which is lower than the inflection point (i.e. $0 < \Psi < \Psi_i$). Eq. 2 shows when θ is less than θ_i, the RSS due to matric suction is zero. In other words, the suction cannot contribute to the RSS of unsaturated soils when it exceeds Ψ_i. This is inconsistent with the experimental observations from modified ring shear tests under constant high suction values. Romero et al. (2014) reported that suction can still contribute to the RSS of unsaturated soils even when suction values are as high as 300 MPa. Therefore, Eq. 2 can only be used when $0 < \Psi < \Psi_i$. However, this is typically the range in which suction values are associated with the changes in the liquid phase flow and is important in conventional geotechnical engineering practice.

Geotechnical engineers understand the importance of RSS in the long-term slope stability analysis of both saturated and unsaturated slopes. However, there are limited case studies in the literature where the RSS concept was considered to interpret the behavior of unsaturated slopes in comparison to saturated soil slopes.

This paper introduces the Outang landslide near the Three Gorges Dam in China which is reactivated recently due to the combined influence of rainfall infiltration and the Yangtze River water level variation at the slope toe. A series of direct shear test results were reported to study the RSS behaviors of the saturated and unsaturated specimens. Based on the RSS parameters, a series of slope stability analysis were conducted using commercial software Geoslope. The results of the study are used to interpret rationally the Outang landslide behavior at residual state conditions.

2 SITE INVESTIGATION STUDIES

2.1 Study area

The investigated Outang landslide is in Anping, Fengjie, China, which is about 177 km away from the Three Gorges Dam. The annual mean temperature and mean precipitation are 16.3 ℃ and 1147.9 mm, respectively. The total annual precipitation is 1636.3 mm. Seventy percent of total annual precipitation occurs between the months of May and September.

The studied landslide is on the south bank of the Yangtze River, inclined from the South to the North. The Yangtze River flows in front of the slope toe, as shown in Figure 2. The water level of the Yangtze River varies between 145 m and 175 m, periodically every year.

2.2 Description of Outang landslide

The length of the studied slope is about 1800 m. The relative difference in elevation between the slope crest and toe is about 600 m. The average gradient of the slope surface is 1:25. The average thickness of the sliding mass is about 50.8 m.

A series of site investigations have been conducted to study the slip surface of the landslide (Dai 2016). The investigation results indicated the sliding mass moved along two weak zones (i.e. R1 and R3 shown in Figure 2) sandwiched between the sliding mass and bedrock. The old landslide has occurred tens of thousands of years ago in three stages, which was estimated with the aid of electron spin resonance (ESR) tests (shown in Figure 2).

Recently, Three Gorges Dam was constructed to the east of the Outang landslide and began to store water since 2003. The Outang landslide performance has been significantly influenced due to the recent construction of

Three Gorges Dam. Dai (2016) reported from field observation results that the old landslide has started to deform again. Firstly, large displacements of sliding mass have been found at some monitoring points. More than 106 cracks were observed on the ground and most of them occurred at the first-stage landslide. The second-stage landslide was still relatively stable. However, settlements of roads, and cracks on the ground was observed every year since 2003 in the third-stage landslide during the rainy season. Thus, it can be concluded that the Outang landslide has been locally reactivated.

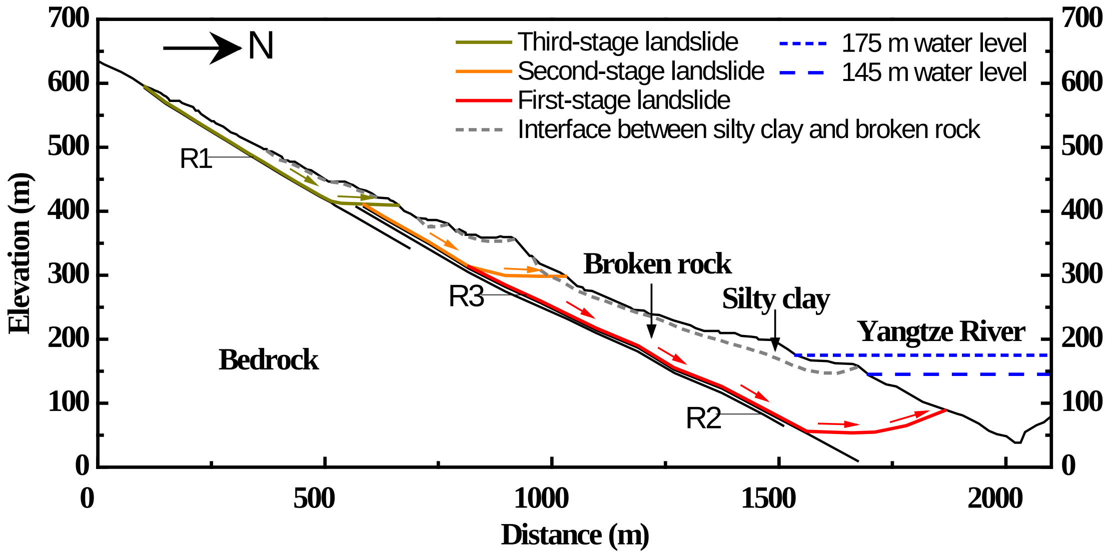

Figure 2 Typical cross section of the Outang landslide (modified after Dai, 2016)

2.3 Rainfall and Yangtze River water level data

Figure 3 summarizes the rainfall data along with the variation of the Yangtze River water level from December 1st, 2010 to December 1st, 2014. Two typical variation curves of the ground surface displacement of the third-stage landslide from May 2012 to December 2014 are also presented in Figure 3. This relationship provides valuable information between the deformation behavior of the landslide and the variation of hydraulic/climatic condition that can be used in the Outang landslide investigation. Dai (2016) reported this data.

From Figure 3, it can be found the precipitation varied periodically during the measurement period (Dec 1st, 2010 – Dec 1st, 2014). The water level of the Yangtze River can be regulated by the Three Gorges Reservoir floodgates. Every year the water level was decreased to a lower value during the rainy season to alleviate possible floods. Therefore, the water level of the Yangtze River also varied periodically based on the annual precipitation.

A significant increase in ground surface displacement was observed from May to September in 2012 and 2014, respectively. However, the increase was much smaller during the same period of 2013. These comparison studies suggest that the displacement variation was consistent with the variation in the precipitation rate. The variation of the water level of the Yangtze River was almost the same every year (i.e. from 175m to 145m). However, the precipitation rate is significantly higher from May to September in 2012 and 2014 than that in the same period during 2013. Therefore, it is reasonable to conclude that the displacement of the studied landslide can be attributed to the combined effect of the precipitation and water level variation.

2.4 Material properties

The site investigation studies have shown that the sliding mass of the Outang landslide has two layers. The surface layer of the sliding mass is a 3 – 20 m layer of silty clay with gravels. An underlying layer is a 10 – 85 m broken rock layer. As shown in Figure 2, three weak zones (R1, R2 and R3) are sandwiched between the sliding mass and bedrock. The site investigation results show the sliding mass moved along the R1 and R3 weak zone. For this reason, only soils in those two weak zones were studied. R1 is a 10 – 35 cm claystone layer. R3 is a 40 – 70 cm clay layer.

Dai (2016) collected several undisturbed soil samples from the silty clay layer, R1 and R3 weak zone. A series of laboratory tests were conducted to determine the physical and shear strength properties of the soils. The physical properties of those soils are summarized in Table 1. The degree of saturation of the natural samples shown in Table 1 was calculated by using the water content and density values. A series of consolidated undrained direct shear tests were conducted on both the natural and saturated soil samples of R1 and R3. In addition, a series of quick undrained direct shear tests were conducted on the natural and saturated soil samples of silty clay. The residual shear strength parameters are also summarized in Table 1.

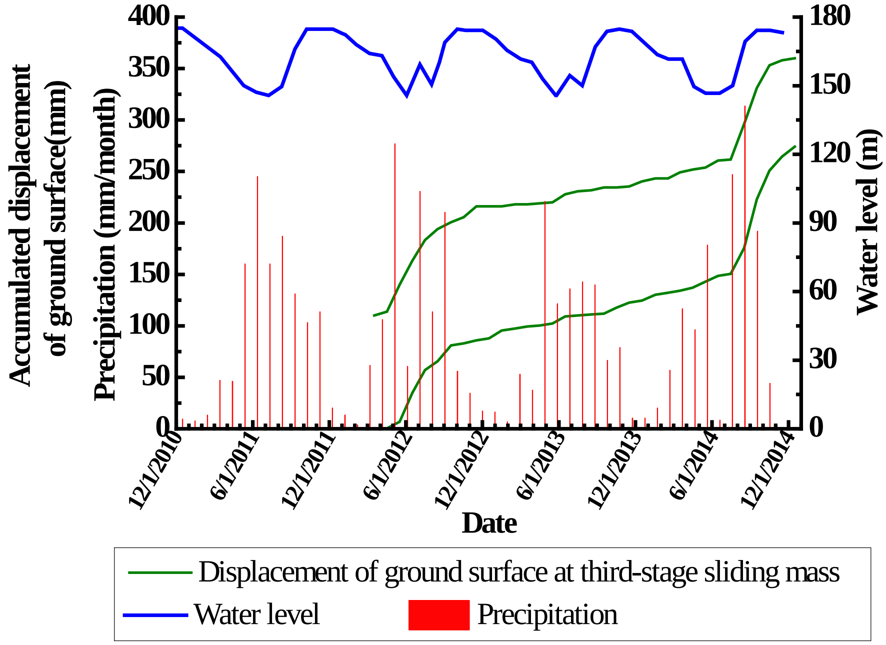

Figure 3 Variation of the Yangtze River water level, precipitation and accumulated displacement of ground surface (modified after Dai, 2016)

Table 1 Physical and mechanical properties of soils (summarized from Dai, 2016)

	Plasticity index	Liquid index	Specific gravity	Natural specimen (Unsaturated) Water content (%)	Density (kg/m^3)	Degree of saturation (%)	c_r (kPa)	ϕ_r (º)	Saturated specimen Water content (%)	Density (kg/m^3)	c_r (kPa)	ϕ_r (º)
Silty clay	12.3	-0.02	-	0.05	2040	-	27.0	11.3	21.63	2070	21.6	9.2
R3	11.1	0.17	2.70	19.48	2070	94.18	27.8	11.5	20.50	2080	24.2	9.3
R1	10.7	0.15	2.71	18.00	2070	89.53	29.0	12.9	19.80	2100	24.7	9.5

3 SLOPE STABILITY ANALYSES

3.1 Schematic of slope used for numerical modelling

A series of numerical modelling studies were conducted based on the RSS parameters using the commercial software Geostudio. Figure 4 presents the numerical model of the landslide. In this numerical model, several assumptions were made to simplify the analyses. Firstly, a simplified slope surface was used in the numerical model ignoring some minor changes in the gradient. Secondly, R2 was neglected in the numerical model since the slip surface did not go through it. The thickness of R1 and R3 were assumed equal to 0.5 m. Lastly, one slip surface was used in the numerical model to replace the slip surfaces which was generated in three stages.

3.2 Calculation procedures

In this numerical model, the combined influence of rainfall infiltration and variation of the water table of the Yangtze River were simulated. The variation of the FOS of the slope with time under the combined influence of these two factors was studied. Three steps were involved in the numerical analysis that can be described as follows:

(1) Steady-state seepage analysis: The boundary conditions on the left boundary and the slope surface below the water level of the Yangtze River (175 m) were set as the constant total head boundary condition. Then, a steady-state seepage analysis was conducted using Seep/W to simulate the pore water pressures in the slope under no precipitation and variation of the water level.

(2) Transient seepage analysis: Based on the numerical model in Step (1), a specific boundary condition was applied on the slope surface to model the precipitation

and variation of the water level. Then, a transient seepage analysis was conducted to calculate the pore water pressures in the slope at different times.

(3) Slope stability analysis: Based on the numerical model in Step (2), the values of FOS of the slope at different times was calculated using the Slope/W and RSS parameters.

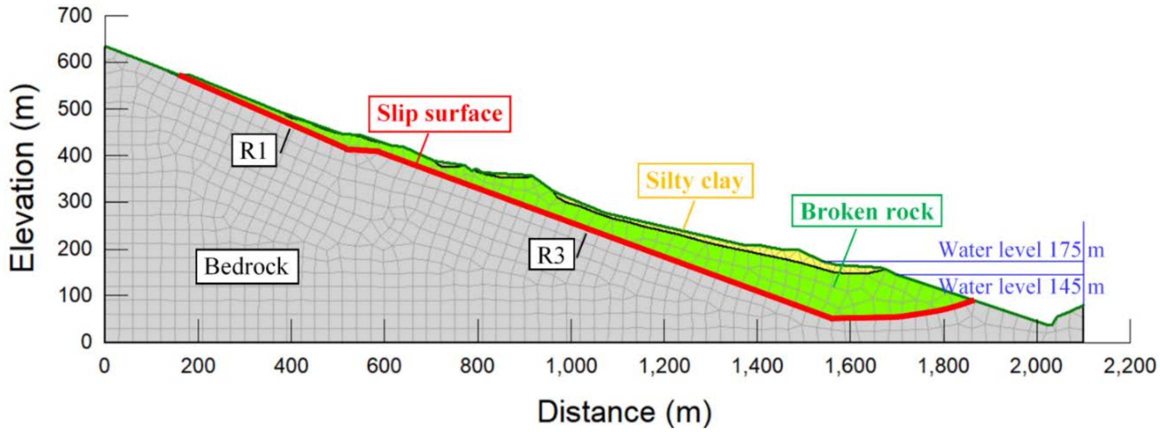

Figure 4 Schematic of the slope used in the numerical modelling

3.3 Boundary conditions

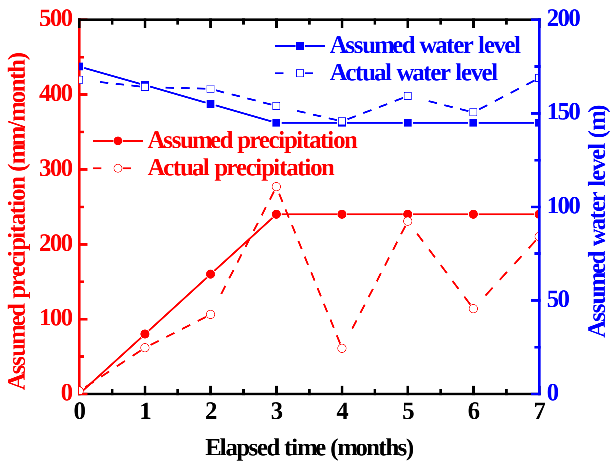

Figure 5 Variation of actual and assumed values of precipitation and Yangtze River water level used in the numerical model (Feb 2012 – Sep 2012)

The unit flux on the bottom and right boundary was set as 0 m/s; i.e. no flow occurred on those two boundaries. Dai (2016) suggested the total head on the left boundary was constant at 525 m.

In the steady-state seepage analysis, the total head on the slope surface below the elevation of 175 m (i.e., the highest water level of the Yangtze River) was set as 175 m.

In the transient seepage analysis, the actual hydraulic/climatic condition was simulated by using the boundary conditions on the slope surface. From Figure 3, it can be found that both the precipitation and water level of the Yangtze River varied periodically with time. Thus, only a representative period of one year (Feb 2012 – Feb 2013) was selected for the study. Additionally, during the wet season of this period, the shear strength decreased due to the rainfall infiltration and the seepage force increased due to the decrease in the water level. The combined influence of water level variation and precipitation might accelerate the slope failure. This means the wet season should be considered as the vulnerable period. Therefore, only the hydraulic/climatic condition for seven months (i.e., Feb 2012 – Sep 2012) was studied in this research. Figure 5 presented the actual and assumed values of precipitation and water level variation.

The unit flux on the slope surface above the elevation of 175 m was defined as a function of the elapsed time as shown in Figure 5. The precipitation increased linearly from 0 to 240 mm/month within first three months. Then, it was constant at 240 mm/month from the 3rd to 7th month. The total head on the slope surface below the elevation of 175 m was also defined as a function of the elapsed time as shown in Figure 5. The total head decreased linearly from 175 m to 145 m within the first three months. Then, it was constant at 145 m from the 3rd to 7th month.

3.4 Material properties

In this numerical model, five types of materials were used, including surface silty clay, claystone zone R1, clay zone R3, broken rock and bedrock (Figure 4). Mohr-Coulomb model was used for all those materials. The hydraulic and shear strength parameters of those materials are described below.

The RSS parameters shown in Table 1 were used for the silty clay, R1 and R3. Dai (2016) did not provide the effective RSS parameters for those materials. The parameters of R1 and R3 were derived from consolidated undrained direct shear test results. The parameters of silty clay were derived from quick undrained direct shear test results. By using this approach, the magnitudes of FOS will be underestimated. However, the research focus in this paper is directed on the slope stability considering the RSS behaviors. Although effective shear strength parameters were not used, the trends in variation of FOS of the simulated slope with time will be similar with that calculated using effective RSS parameters. In other words, the slope behavior can still be analyzed considering the RSS.

Dai (2016) did not provide experimental results for the shear strength parameters of the broken rock and bedrock and the hydraulic properties of all those five materials. However, He conducted several numerical modelling studies of the Outang landslide. A series of values of the peak shear strength parameters and hydraulic properties have been suggested for all the five materials. In this numerical model, the RSS parameters of the broken rock and bedrock were assumed equal to the PSS parameters, which were suggested by Dai (2016) (shown in Table 2). The slip surface only passed through the R1 and R3 weak zone. This means the shear strength parameters of the broken rock and bedrock did not influence the FOS of the slope. Therefore, the assumption will not influence the FOS.

Table 2 Shear strength parameters in numerical model (summarized from Dai 2016)

	c_p' (kPa)	ϕ_p' (°)	c_r' (kPa)	ϕ_r' (°)
Broken rock	70	16.2	70	16.5
Bedrock	700	42	700	42

Table 3 Parameters of SWCC (summarized from Dai 2016)

	a	n	m	θ_s	θ_r	Ψ_i (kPa)
Silty clay	10.65	1.40	0.81	0.32	0.059	20
Broken rock	9.12	1.73	0.76	0.27	0.051	16
R1 and R3	9.07	1.53	0.59	0.30	0.094	20
Bedrock	9.81	1.46	0.70	0.05	0.012	20

The SWCC and permeability functions of those materials also used the values suggested by Dai (2016). The same SWCC and permeability functions were used for the R1 and R3 weak zones, since both of them were clays. The SWCC were fitted by using the equation proposed by Fredlund & Xing (1994). The related parameters are summarized in Table 3, where θ_s and θ_r are the saturated and residual volumetric water content. The permeability functions are presented in Figure 6.

The prediction models for RSS of unsaturated soils (e.g. Eq. 1 and Eq. 2) were described in the earlier sections. Dai (2016) did not provide the apparent SWCC of the sheared specimens. In addition, the seepage analysis in the present study showed the suction in the slope could reach as high as 800 kPa. This means in some parts of the slope the suction values may be greater than Ψ_i. Therefore, Eqs. 1 and 2 should not be used as it is. Thus, a model was postulated in this research to calculate the RSS analogous with the PSS prediction model proposed by Vanapalli et al. (1996) (i.e. Eq. 3). The model can be expressed as Eq. 4.

$$\tau = c' + (\sigma_n - u_a)\tan\phi' + (u_a - u_w)\left(\frac{\theta - \theta_r}{\theta_s - \theta_r}\right)\tan\phi' \qquad [3]$$

$$\tau_r = c_r' + (\sigma_n - u_a)\tan\phi_r' + (u_a - u_w)\left(\frac{\theta - \theta_r}{\theta_s - \theta_r}\right)\tan\phi_r' \qquad [4]$$

Where, (σ_n - u_a) is the net normal stress; (u_a – u_w) is the matric suction; c_r' and ϕ_r' are the RSS parameters of saturated soils; θ_s and θ_r are the saturated and residual volumetric water content.

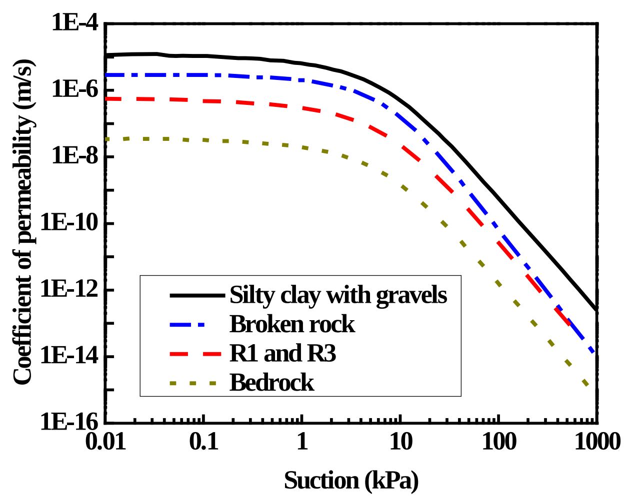

Figure 6 Coefficient of permeability functions for different materials (modified after Dai 2016)

Equation 4 was used to approximate the RSS of unsaturated soils in this research. The parameter, $(\theta - \theta_r)/(\theta_s - \theta_r)$ in this equation describes the reduction in suction contribution at peak state with increasing suction. However, after peak state, some water menisci are destroyed. Thus, the reduction in suction contribution at residual state should be greater than that at peak state. In Eq. 4, $(\theta - \theta_r)/(\theta_s - \theta_r)$ is still used to describe the reduction in suction contribution. It tends to underestimate the reduction in suction contribution at residual state; i.e., Eq. 4 tends to overrate the RSS.

Finally, based on the RSS, the FOS of the slope was calculated by using Morgenstern-Price method (Geoslope user's guide 2012). The slip surface as shown in Figure 4 was specified manually and used in the slope stability analyses,

4 ANALYSES OF RESULTS

Figure 7 presents the variation of FOS at residual state (FOS_R) with time under the combined influence of precipitation and water level variation. It can be found that FOS_R decreased almost linearly within the first three months with a maximum value of 6.6%. In the following four months, the decrease in FOS_R was much slower (0.66%).

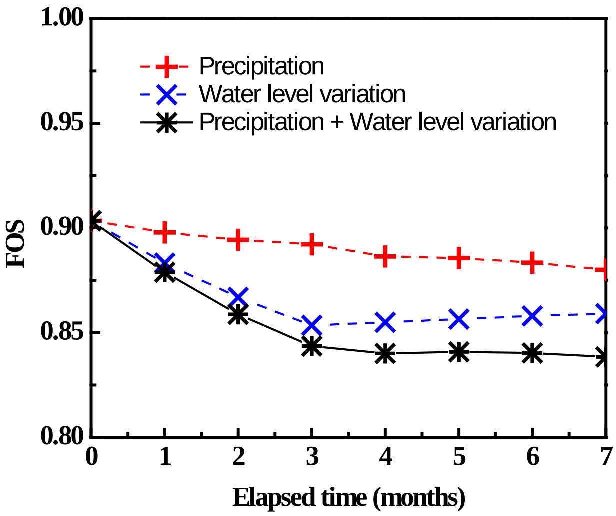

Figure 7 Variation of FOS at residual state with time under different hydraulic/climatic conditions

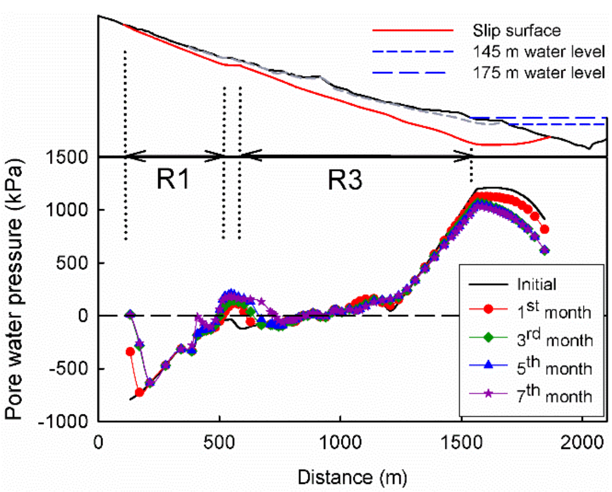

Figure 8 Pore water pressure profiles along slip surface under the combined influence of precipitation and water level variation

In order to study the mechanisms associated with the landslide reactivation, soil suction profiles along the slip surface under the combined influence of the precipitation and water level variation are presented in Figure 8. A sketch of the slope (shown in Figure 4) is reproduced in Figure 8 to indicate the positions where suctions were obtained. The reactivation of the landside can be attributed to two reasons.

The first reason is associated with the suction decrease caused by rainfall infiltration. The rainfall infiltration can cause an increase in the pore water pressure. Conversely, the decrease in water level can cause a decrease in pore water pressure. From Figure 8, it can be found the pore water pressures only increased (i.e. the suction decreased) on the slip surface at the top of R1 and the connection between R1 and R3. This means the rainfall infiltration mainly influenced these two zones. Such a behavior may be attributed to the slip surface being shallow at the top of R1 (Figure 8). The infiltrated rainfall can reach the slip surface within a short time period. At the connection between R1 and R3, the bedrock is almost horizontal (Figure 8); thus, the infiltrated rainfall tended to accumulate above the bedrock. Once the suction decreased on the slip surface, the RSS of the slide zone soils reduced as a result. Therefore, the FOS_R decreased.

The second reason is the seepage force increase caused by decrease in the water level. From Figure 8, it can be found that the pore water pressures decreased only on the slip surface near the river. The pore water pressures decreased on this part of slip surface; however, they were still positive values. Therefore, the decrease in the water level did not influence the RSS of the slide zone soils. However, with decreasing water level, the difference between the water levels at the rear and front part of the slope increased. Consequently, the seepage force increased as a driving force in the sliding mass. Due to this reason, the FOS_R decreased.

In order to further study the influence of precipitation and water level decrease, two more numerical modelling studies were conducted, which considered the influence of precipitation and water level decrease, separately. The variations of FOS_R with time in those two scenarios were presented in Figure 7. In the first three months, the decrease in FOS_R caused by the water level decrease was much greater than that caused by the rainfall infiltration. This is because the slip surface which was influenced by the rainfall infiltration was far above the phreatic line. This means the matric suction on this part of slip surface was high and the volumetric water content was low. The contribution of the matric suction to RSS is lower than that of the overburden pressure. Thus, the reduction in matric suction contribution can only cause a relatively small decrease in the RSS. In addition, the extent of the zones which were influenced by the rainfall infiltration was still limited. On most part of the slip surface, the RSS was not influenced by the rainfall infiltration. The decrease in FOS_R caused by the rainfall infiltration was relatively small. In other words, it was the decrease in Yangtze River water level that had a dominant contribution to the reduction in FOS_R within the first three months. From the 3rd to 7th month, the continuous precipitation caused a further decrease in FOS_R. However, FOS_R increased slightly for the scenario where only the water level decrease was considered. This means, once the water level attains a relatively constant value, the rainfall infiltration should be the dominant factor that contributes to the reduction in FOS_R.

In addition, it can also be found that the FOS_R was less than 1 initially when the precipitation and water level decrease did not start. This result is inconsistent with the field observations which indicated that the slope was stable before the precipitation and water level variation occurred. The inconsistency can be attributed to an assumption in the numerical model that the RSS parameters were used throughout the slope, which did not fit the actual case. In reality, the magnitude of shear strength should depend on the level of deformation. Initially, when no deformation occurs, the shear strength of soils should be interpreted based on PSS parameters. After the precipitation increases and Yangtze River water level decreases, large deformations occur in some zones of the slope. As a result, in those zones with large deformations, the shear strength is likely to be reduced to the RSS. The shear strength in other zones might be somewhere between the PSS and RSS depending on the magnitudes of deformation. Therefore, different values of shear strengths should be used in different zones of the slope according to the deformation level for reliably determining the FOS. If the RSS is used throughout the slope, the FOS will be underestimated. However, this approach provides a conservative value of FOS for the slope stability analysis.

5 SUMMARY

In this paper, a reactivated landslide near the Three Gorges Dam in China was revisited and analyzed. A series of site investigation and direct shear test results were reported to study the progressive failure behaviors of the landslide. The landslide was reactivated by the combined influence of the precipitation and Yangtze River water level variation. A series of numerical modeling were conducted using Geoslope to study the slope stability of the landslide based on the residual shear strength. The key results are summarized below:

(1) FOS_R decreased during the seven-month study period. This can be attributed to the reduction in the RSS of the slide zone soils caused by the rainfall infiltration and the increase in the seepage force caused by the Yangtze River water level decrease.

(2) During the period of the water level variation, the water level decrease should be the dominant factor that contributed to a significant reduction in FOS_R. Once the water level reached a relatively constant value, precipitation became the dominant factor contributing to the FOS_R reduction; however, the reduction rate was relatively smaller.

(3) In reality, different values of shear strengths should be used in different zones of the slope according to the deformation level. In other words, the RSS should be only used in the zones with large deformations; however, the values of shear strength between the PSS and RSS should be used in other zones depending on the magnitudes of deformation. If the RSS was used throughout the slope, the FOS would be underestimated. The slope stability analyses in this study are based on RSS; for this reason, they provide conservative results.

6 REFERENCES

Dai, Z.W. 2016. Study on the deformation and failure mechanism of Outang landslide in the Three Gorges Reservoir Region, China. *Ph.D. thesis*, Chang'an University, Xi'an, Shanxi, China. (in Chinese)

Fredlund, D.G. and Xing, A. 1994. Equations for the soil-water characteristic curve, *Canadian Geotechnical Journal*, 31: 521-532.

GeoSlope International Ltd. 2012. Stability modeling with SLOPE/W: an engineering methodology. *GEO-SLOPE International Ltd*. Calgary, Alberta, Canada.

Hoyos, L.R., Velosa, C.L. and Puppala, A.J. 2014. Residual shear strength of unsaturated soils via suction-controlled ring shear testing, *Engineering Geology*, 172, 1-11.

Infante Sedano, J.A. and Vanapalli, S.K. 2011. Experimental investigation of the relationship between the critical state shear strength of unsaturated soils and the soil-water characteristic curve, *International Journal of Geotechnical Engineering*, 5(1), 1-8.

Locat, A., Jostad, H.P. and Leroueil, S. 2013. Numerical modeling of progressive failure and its implications for spreads in sensitive clays, *Canadian Geotechnical Journal*, 50(9), 961-978.

Lupini, J.F., Skinner, A.E. and Vaughan, P.R. 1981. The drained residual strength of cohesive soils, *Geotechnique*, 31(2), 181-213.

Potts, D.M., Kovacevic, N. and Vaughan, P.R. 1997. Delayed collapse of cut slopes in stiff clay, *Géotechnique*, 47(5): 953-982.

Qi, S. and Vanapalli, S.K. 2016. Influence of swelling behavior on the stability of an infinite unsaturated expansive soil slope, *Computers and Geotechnics*, 70, 154-169.

Romero, E., Vaunat, J. and Merchán, V. 2014. Suction effects on the residual shear strength of clays, *Journal of Geo-Engineering Sciences*, 2(1-2), 17-37.

Skempton, A.W. 1964. Long-term stability of clay slopes, *Géotechnique*, 14(2), 77-102.

Vanapalli, S.K., Fredlund, D.G., Pufahl, D.E. and Clifton, A.W. 1996. Model for the prediction of shear strength with respect to soil suction, *Canadian Geotechnical Journal*, 33(3), 379-392.

Widger, R.A. and Fredlund, D.G. 1979. Stability of swelling clay embankments, *Canadian Geotechnical Journal*, 16(1), 140-151.

Yang, K.H., Uzuoka, R., Lin, G.L. and Nakai, Y. 2017. Coupled hydro-mechanical analysis of two unstable unsaturated slopes subject to rainfall infiltration, *Engineering Geology*, 216, 13-30.

Yang, X. and Vanapalli S.K. 2018. Slope stability analysis of a slope based on the peak and the residual shear strength of unsaturated soils. *Proceedings of 7th International Conference on Unsaturated Soils (UNSAT 2018)*, Hong Kong, China.